Metallophysics and Advanced Technologies
Металофіз. новітні технол.
Metallofiz. Noveishie Tekhnol.
2026, vol. 48, No. 5, pp. 449–462
https://doi.org/10.15407/mfint.48.05.0449
Reprints available directly from the publisher

PACS numbers: 07.85.-m, 61.05.cc, 61.05.cp, 61.72.Dd, 61.72.J-, 61.72.Lk

Characterization of the Defect Structure of Crystalline Compounds by the Total Integrated-Reflectivity Method

V. B. Molodkin, I. M. Fodchuk*, A. R. Kuzmin*, V. V. Dovganyuk*, I. I. Hutsuliak*, M. S. Solodkyi*, R. A. Zaplitnyy*, Ya. D. Garabazhiv*, and V. V. Lizunov

G. V. Kurdyumov Institute for Metal Physics, N.A.S. of Ukraine,
36 Academician Vernadsky Blvd.,
UA-03142 Kyiv, Ukraine
**Yuriy Fedkovych Chernivtsi National University,*
2 Kotsyubynsky Str.,
UA-58002 Chernivtsi, Ukraine

The defect structure of crystalline compounds is investigated using the total integrated-reflectivity method. For interpretation of the experimental data, a generalized dynamical theory of x-ray diffraction is applied to real crystals containing randomly distributed microdefects of various types and a disturbed surface layer. The dynamics of the concentration and size variations are analysed for several types of interconnected dominant defects, including spherical and disk-shaped clusters, as well as dislocation loops.

Key words: total integrated reflectivity, high-resolution x-ray diffractometry, dynamical theory, kinematical theory, diffraction curves, crystalline compounds.

Досліджено дефектну структуру кристалічних сполук методою повної інтеґральної відбивної здатности. Для інтерпретації експериментальних даних використано узагальнену динамічну теорію дифракції Х-променів

Corresponding author: Ihor Mykhaylovych Fodchuk
E-mail: ifodchuk@ukr.net

Citation: V. B. Molodkin, I. M. Fodchuk, A. R. Kuzmin, V. V. Dovganyuk, I. I. Hutsuliak, M. S. Solodkyi, R. A. Zaplitnyy, Ya. D. Garabazhiv, and V. V. Lizunov, Characterization of the Defect Structure of Crystalline Compounds by the Total Integrated-Reflectivity Method, *Metallofiz. Noveishie Tekhnol.*, **48**, No. 5: 449–462 (2026). DOI: 10.15407/mfint.48.05.0449

у реальних кристалах з хаотично розподіленими мікродефектами різних типів і порушеним приповерхневим шаром. Досліджено динаміку зміни концентрацій і розмірів декількох типів взаємопов'язаних домінувальних дефектів (сферичні та дископодібні кластери, дислокаційні петлі).

Ключові слова: повна інтеґральна відбивна здатність, високороздільча Х-променева дифрактометрія, динамічна теорія, кінематична теорія, криві дифракційного відбивання, кристалічні сполуки.

(Received 3 March, 2026; in final version, 16 April, 2026)

1. INTRODUCTION

This article is dedicated to the memory of Prof. V. B. Molodkin, Corresponding Member of the National Academy of Sciences of Ukraine.

Over the recent decades V. B. Molodkin and his colleagues working at G. V. Kurdyumov Institute for Metal Physics, NAS of Ukraine have demonstrated the possibility of radically increasing the sensitivity and information capacity of defective structure diagnostics. This was achieved through the application of dynamical diffraction, the theoretical foundations of which were established by V. B. Molodkin [1–4].

Modern non-destructive structural diagnostics is based on the experimental study of how structural imperfections influence the diffraction scattering pattern of the investigated object using various x-ray wavelengths, followed by the structural characteristics decoding based on the pattern parameters. The kinematical theory of Bragg and diffuse scattering in crystals with defects, developed by M. O. Krivoglaz, has been and remains the theoretical basis for quantitative research on defect characteristics and their distribution [5, 6]. However, the single-scattering approximation, which underlies the kinematical theory, leads to significant limitations in its application. Specifically, the kinematical theory is effective for polycrystals and single crystals highly distorted by defects, but it becomes largely inapplicable when the dimensions of the crystals and coherent scattering regions exceed the extinction length. In such cases, the theory of multiple dynamical scattering is required [7–9].

Another drawback of the kinematical theory is that it allows for the investigation of defect characteristics only if a single dominant type is present in the crystal. This is due to the fact that the kinematical pattern remains virtually identical across all diffraction conditions; it reflects experimental measurements of the defects' influence on a single scattering pattern, from which characteristics of only one defect type can be determined. Currently, most modern devices are multiparametric, and single-crystal components simultaneously contain multiple types of defects. Furthermore, the sensitivity of kinematical scattering is insufficient for the quantitative diagnostics of even a

single defect type in structurally perfect single crystals. In this case, coherent scattering can be correctly described only within the framework of the dynamical theory of x-ray scattering [10–12], accounting for multiple scattering processes.

In addition, it was predicted and experimentally confirmed by double-axis and triple-axis diffractometry methods that dynamical effects also occur with diffuse x-ray scattering near Bragg reflections from imperfect single crystals [13–15]. In the case of Bragg diffraction geometry, these effects cause a significant reduction in diffuse scattering intensity within the total reflection region (the extinction effect) and its redistribution near the Bragg peak (anomalous transmission and absorption effects) [8, 9]. During the dynamical x-ray scattering in crystals with defects, much like in the dynamical theory for ideal crystals, the boundary conditions and diffraction geometry of the investigated crystal exert a substantial influence on the distribution and magnitude of the diffracted x-ray intensity, in contrast to the kinematical theory. Furthermore, the thickness of the crystal and the radiation energy significantly affect the behaviour of diffracted intensities in both perfect and defective crystals. Isolating and utilizing the diffuse scattering component under dynamical diffraction conditions enhances the informative potential of these methods, as diffuse scattering carries the most comprehensive and direct information regarding the structural perfection of the objects. At sufficiently high defect concentrations, they can contribute significantly to the diffuse scattering intensity in the Bragg peak region. A correct description of diffuse scattering is provided by the dynamical theory of x-ray diffraction in crystals with randomly distributed defects.

The primary advantage of angular intensity distributions is the ability to determine the concentration and size of defects, as well as their type (interstitial or vacancy) and the symmetry of the static distortion fields they create. Among these highly informative methods is the total integrated reflectivity (TIR) method, where information about defects is extracted from the full diffraction curves, which represent the distributed scattering intensity. Consequently, when considering relatively perfect single crystals with defects, it is necessary to apply diagnostics based specifically on the dynamical scattering theory [16, 17].

This approach is based on the analysis of the TIR from investigated crystal. In Refs. [18–22], the dislocation structure of crystalline compounds was studied based on the kinematical theory of x-ray scattering. In contrast, the TIR method employs the dynamical theory to obtain more comprehensive information about the defective structure. We have approved this method for crystalline compounds with a well-developed defective structure. Its application enables the estimation of the concentrations and sizes of several defect types, namely, dislocation loops, disk-shaped formations (extended blocks) and spherical

formations (grains). This method allows for the most complete and accurate diagnostics of defects within the bulk of single crystals and the determination of the parameters of disturbed surface layers.

Cadmium telluride CdTe crystalline compounds are widely used in the fabrication of x-ray and γ-ray detectors [23, 24]. However, CdTe crystals are characterized by a well-developed defect structure (various types of dislocations, dislocation loops, foreign phase inclusions, cluster formations, *etc*.), which subsequently has a negative impact on their sensing properties. Although the methods for growing high-perfection crystalline compounds improve every year, the influence of the defect structure on the electrical and spectroscopic properties of detectors remains an ever-present and relevant problem.

In the article, the using of TIR method is illustrated by the example of semiconductor materials. Nevertheless, the appropriateness of using such methods in the researching of metallic single crystals with microdefects is even higher than for semiconductors. This is due to the fact that an approximate description of the effects of radiation scattering (including dynamical effects) in such crystalline compounds can lead not only to a quantitative, but also to a qualitatively incorrect description of the defect structure. For example, the kinematical theory of scattering for single crystals with dislocations assumes a complete absence of a coherent component of the intensity. However, in the dynamical approach, taking into account the effects of multiple scattering, leads to an effective cut-off of the contribution of distant dislocations to the scattering characteristics and, as a result, even with a sufficiently high concentration of dislocations in the crystal, coherent peaks are observed.

This paper presents the results of testing the method of total integrated reflectivity and computer simulation of the defect structure for several types of defects in cadmium telluride crystalline compounds.

2. OBJECTS OF RESEARCH

The objects of research are a set of (111)CdTe crystalline compound samples from Acrorad Co., Ltd., grown by the traveling heater method, with dimensions of $5\times5\times1$ mm^3 [25, 26]. Experimental studies were conducted on a Panalytical Philips X'Pert PRO diffractometer using radiation Cu$K_{\alpha1}$. The divergence of the primary beam and the angular acceptance of the analyser crystal used before the detector is $\Delta\alpha \cong 12''$.

3. TOTAL INTEGRATED REFLECTIVITY METHOD

The generalized dynamical theory of x-ray diffraction in real crystals with randomly distributed microdefects of various types and a dis-

turbed surface layer was used to interpret the experimental results [27]. The best results were obtained for a model containing the following dominant types of microdefects: disk-shaped clusters, small spherical clusters, and dislocation loops. The presence of thermal diffuse scattering was accounted for by scattering on point defects, represented by spherical clusters with sizes equal to the covalent radii of cadmium and tellurium atoms. The strain distribution in the disturbed surface layer was represented by a multistep profile corresponding to the so-called 'layer-by-layer approximation'. Within this approximation, the disturbed layer is represented as a set of sublayers with thickness t_i, in each of which the strain epsilon is constant.

Unlike the kinematical theory, the dynamical theory introduces two additional structurally sensitive parameters (which in several cases are significantly more informative than the Krivoglaz's factor (static Debye–Waller factor E^2): these are the integrated extinction coefficients of the coherent (μ_{ds}^0) and diffuse (μ^*) components of TIR. This provides an opportunity, unavailable in the kinematical case, to determine unambiguously the parameters of several defect types simultaneously using TIR measurements [8, 9].

In the case of a uniform distribution of bounded defects with radius R_0 and concentration c, the following expression is valid [28]:

$$\begin{gathered}\mu_{ds}^0 = cE^2C^2m_0B,\ m_0 = \pi v_c H^2 \left|\chi_{Hr}\right|^2 / (2\lambda^2), \\ B = b_1 + b_2 \ln(e / r_0^2),\ b_1 = B_1 + B_2 / 3,\ b_2 = B_1 + \cos^2\theta_B B_2 / 2,\end{gathered} \tag{1}$$

where $r_0 = R_0/\Lambda$, $\Lambda = \lambda(\gamma_0\gamma_H)^{1/2}/(C\left|\chi_{Hr}\right|)$ is the extinction length, **H** is the diffraction vector, e is the base of the natural logarithm, and it is assumed that $r_0 < 1$.

For spherical clusters: $B_1 = 0$, $B_2 = (4\pi A_{cl}/v_c)^2$, $A_{cl} = \Gamma\varepsilon R_0^3$ is the cluster strength, ε is relative strain at the cluster boundary, and $\Gamma = (1+\nu)/((3(1-\nu))$. For disk-shaped clusters: $B_1 = B_2 = (4\pi A_{cl}/v_c)^2$, $A_{cl} = \Gamma\varepsilon h_p R_p^2$ is the cluster strength. For randomly distributed dislocation loops: $B_1 = 4(\pi b_0^2 / v_c)^2 / 15$, $B_2 = bB_1$, $\beta = (3\nu^2 + 6\nu - 1)/(4(1-\nu^2))$, v_c is the unit cell volume, ν is the Poisson's ratio, and **b** is the Burgers vector.

If $\mu_{ds}^0 << \mu_0$ and $r_0 << 1$, the following approximate relationship is valid [29]:

$$\begin{gathered}\mu^* \approx \mu_{ds}^0 f_\mu(r_0), \\ f_\mu(r_0) = \frac{5 + 2r_0 \ln r_0 - 3r_0/8}{3(1 - \ln r_0)} \text{ for dislocation loops}, \\ f_\mu(r_0) = \frac{4 + r_0 \ln r_0 - 2r_0}{5 - 6\ln r_0} \text{ for dislocation clusters},\end{gathered} \tag{2}$$

The relationship between the Krivoglaz's factor exponent $L_{\text{H}} = -\ln E$ and the defect characteristics is described by the following expressions:

$$L_{\text{H}} \approx 0,5cv_{\text{c}}^{-1}R_0^3(Hb)^{3/2} \text{ for dislocation loops}, \quad (3)$$

$$L_{\text{H}} \approx 0,5cn_0\eta^2(1-\eta^2/100) \text{ for spherical clusters } (\eta^2<<10), \quad (4)$$

$$L_{\text{H}} \approx cn_0\eta^{3/2} \text{ for spherical clusters } (\eta^2<<10),$$

where $n_0 \approx 4\pi R_0^3/3v_{\text{c}}$ is the number of matrix unit cells replaced by a cluster, $\eta = \alpha_0 n_0^{1/3} h$, $\alpha_0 = \Gamma\varepsilon(6\pi^2/n_0)^{1/3}$, ν_0 is the number of atoms in the cubic matrix cell, $h = Ha/2\pi$, and a is the lattice constant.

Through the parameters E, μ_{ds}^0, and μ^*, the TIR value R_{i} is linked to the defect characteristics (c, R_0, ε, b).

In the case of arbitrary (asymmetric) Bragg diffraction geometry, the expression for the TIR, which combines the limiting cases of 'thin' ($\mu_0 l << 1$) and 'thick' ($\mu_0 l >> 1$) crystals, is as follows:

$$R_{\text{i}} = R_{\text{i}}^{\text{dyn}} PE + R_{\text{i}}\Pi(1-E^2), \quad (5)$$

$R_{\text{i}}^{\text{dyn}} = 16CQ\Lambda/3\pi\gamma_0$, $R_{\text{i}} = C^2Qt/\gamma_0$ is the TIR of a perfectly mosaic crystal,

$$\Pi(\mu^*, t) = \begin{cases} (2(\mu_0+\mu^*)t/\gamma)^{-1}, & \mu_0 t >> 1, \\ (1+(\mu_0+\mu^*)t/\gamma)^{-1}, & \mu_0 t < 1,\ t >> \Lambda_B, \end{cases}, \quad (6)$$

$1/\gamma = (1/\gamma_0 + 1/|\gamma_{\text{H}}|)/2$, $\Lambda_B = l(/\gamma_0|\gamma_{\text{H}}|)^{1/2}/(2\pi C\chi_{\text{Hr}}) = L/2\pi$, $P = 1 - 3\pi s/4$ with $s = (\mu_0 + \mu_{\text{ds}}^0)\Lambda E/\gamma C$, $s << 1$, P is the polarization factor, $Q = (\pi|\chi_{\text{Hr}}|^2)/(\lambda\sin(2\theta))$ is the reflectivity per path length unit, χ_{Hr} is the real part of the Fourier component of the crystal polarizability, t is the crystal thickness, γ_0, γ_{H} are the direction cosines of the wave vectors of the plane wave incident on the crystal and the diffracted wave, respectively, relative to the inward normal to the entry surface, and μ_0 is the linear photoelectric absorption coefficient.

Here, the integrated effective absorption coefficients μ_{ds}^0 and μ^* are described by the approximate expressions (1), (2) under conditions $\mu_{\text{ds}}^0 << \mu_0$ and $R_0 << \Lambda$.

4. RESEARCH RESULTS

Experimental dependences of TIR, normalized on the reflectivity of ideal crystal, on the reflection order (extinction thickness Λ_{hkl}) are shown in Fig. 1. These dependences are non-monotonic. Samples Nos. 2 and 4 exhibit higher TIR values than sample No. 2; notably, the maximum increase in reflectivity is observed at lower reflection orders for

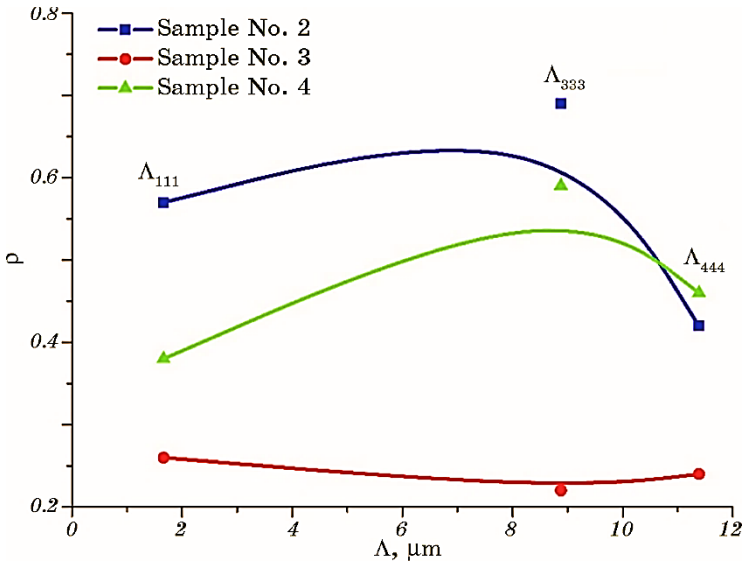

Fig. 1. Dependences of the normalized TIR ρ on the reflection order (extinction thickness values) for a set of samples.

sample No. 2. The calculation of the normalized TIR was performed with a precision of 0.01, meaning the calculated dependences of the normalized TIR on the reflection order will have same shape.

We considered several possible combinations of microdefects with different sizes and concentrations present in the investigated crystals [30]: disk-shaped clusters—relatively large CdTe grains surrounded by dislocation loops of corresponding sizes, and small spherical clusters—

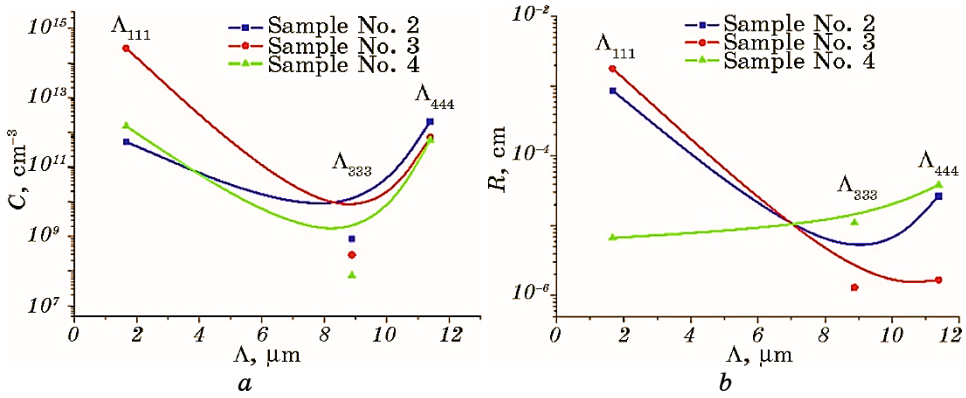

Fig. 2. Dependences of concentrations (*a*) and sizes (*b*) of dislocation loops on the reflection order.

TABLE 1. Values of concentrations C and sizes R of dislocation loops depending on the order of reflection.

Sample		Reflection		
		111	333	444
2	C, cm^{-3}	$5.3 \cdot 10^{11}$	$8.5 \cdot 10^{8}$	$2.1 \cdot 10^{11}$
3		$2.7 \cdot 10^{14}$	$2.9 \cdot 10^{8}$	$7.2 \cdot 10^{11}$
4		$1.5 \cdot 10^{12}$	$7.3 \cdot 10^{7}$	$5.6 \cdot 10^{11}$
2	R, cm	$8.7 \cdot 10^{-4}$	$1.3 \cdot 10^{-6}$	$2.6 \cdot 10^{-5}$
3		$1.8 \cdot 10^{-3}$	$1.3 \cdot 10^{-6}$	$1.6 \cdot 10^{-6}$
4		$6.7 \cdot 10^{-6}$	$1.1 \cdot 10^{-5}$	$3.8 \cdot 10^{-5}$

small CdTe grains located in the spaces between large grains; disk-shaped clusters—relatively large CdTe grains, and dislocation loops.

The best agreement between the experimental and theoretical TIR dependences (Fig. 1, $\rho = \rho_{exp} \approx \rho_{teor}$, the deviation does not exceed 1%) was obtained for the first model, which assumes the presence of three types of dominant defects in the crystal. This allowed for the determination of the characteristics (concentration and size) of the dominant defects in the crystals (Figs. 2–4, Tables 1–3).

Samples Nos. 2–4 exhibit several characteristic features on $C(\Lambda_{hkl})$ dependences (Figs. 2–4, *a*). Specifically, the concentration of dislocation loops for all samples (Fig. 2) comparing to the control sample decreases sharply from the surface to a depth of ≅ 9 μm, followed by an increase. The decrease in concentration at a depth of 9 μm is associated

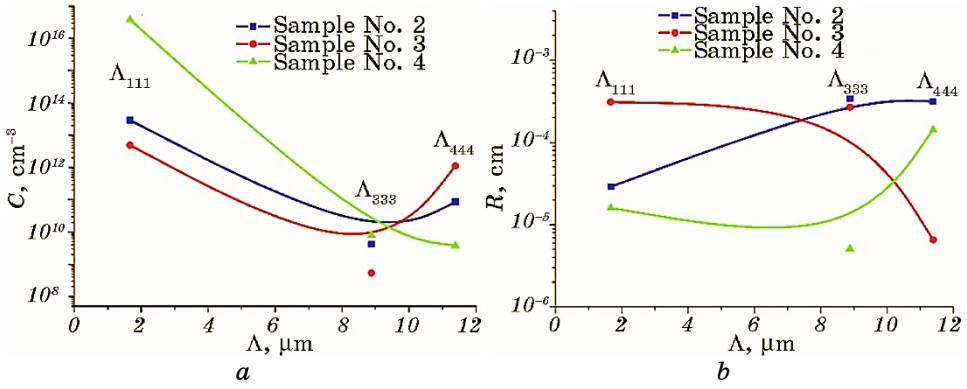

Fig. 3. Dependences of concentrations (*a*) and sizes (*b*) of disk-shaped clusters on the reflection order.

TABLE 2. Values of concentrations C and sizes R of disk-shaped clusters *versus* the reflection order.

Sample		Reflection		
		111	333	444
2	C, cm^{-3}	$2.9 \cdot 10^{13}$	$4.2 \cdot 10^{9}$	$8.5 \cdot 10^{10}$
3		$4.9 \cdot 10^{12}$	$5.4 \cdot 10^{8}$	$1.1 \cdot 10^{12}$
4		$3.8 \cdot 10^{16}$	$8.1 \cdot 10^{9}$	$3.8 \cdot 10^{9}$
2	R, cm	$2.9 \cdot 10^{-5}$	$3.4 \cdot 10^{-4}$	$3.2 \cdot 10^{-4}$
3		$3.1 \cdot 10^{-4}$	$2.7 \cdot 10^{-4}$	$6.6 \cdot 10^{-6}$
4		$1.6 \cdot 10^{-5}$	$5.1 \cdot 10^{-6}$	$1.4 \cdot 10^{-4}$

with a possible ordering of the structure, followed by its subsequent disordering deeper into the crystal. This is confirmed by the uniformity of the dislocation loop sizes at this extinction depth in samples Nos. 2 and 3. Sample No. 4 is characterized by a nearly monotonic behaviour of the $R(\Lambda_{hkl})$ dependence.

A somewhat different trend is observed in the $C(\Lambda_{hkl})$ dependences for disk-shaped clusters. Samples Nos. 2 and 3 are characterized by an inflection point in the region of the (333) reflection, followed by an increase toward (444). Sample No. 4 has a monotonic decrease with increasing Λ_{hkl}. A notable feature is that at the depth of Λ_{333}, the concentration values for all samples remain within the same order of magnitude. A completely different behaviour is observed for the size dependences $R(\Lambda)$. Sample No. 2 exhibits a monotonic curve within a single

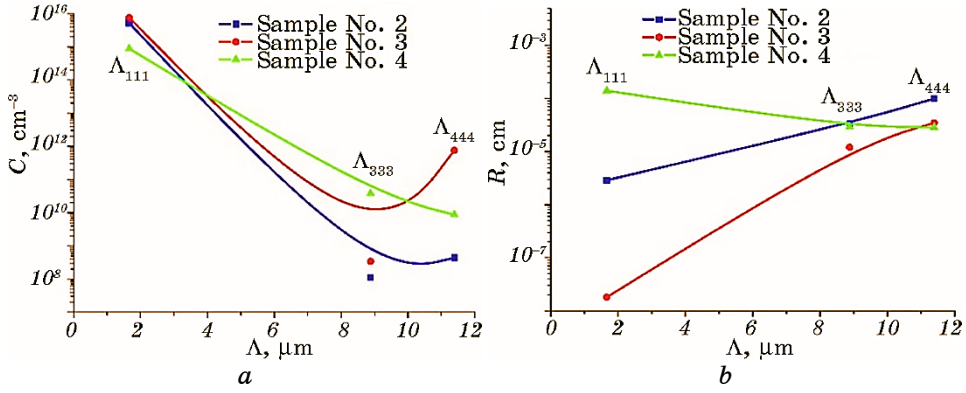

Fig. 4. Dependences of concentrations (*a*) and sizes (*b*) of spherical clusters on the reflection order.

TABLE 3. Values of concentrations C and sizes R of spherical clusters *versus* the reflection order.

Sample		Reflection		
		111	333	444
2	C, cm^{-3}	$5.2 \cdot 10^{15}$	$1.1 \cdot 10^{8}$	$4.4 \cdot 10^{8}$
3		$7.5 \cdot 10^{15}$	$3.4 \cdot 10^{8}$	$7.6 \cdot 10^{11}$
4		$8.8 \cdot 10^{14}$	$3.8 \cdot 10^{10}$	$8.7 \cdot 10^{9}$
2	R, cm	$2.9 \cdot 10^{-6}$	$3.4 \cdot 10^{-5}$	$9.9 \cdot 10^{-5}$
3		$1.8 \cdot 10^{-8}$	$1.2 \cdot 10^{-5}$	$3.5 \cdot 10^{-5}$
4		$1.4 \cdot 10^{-4}$	$2.9 \cdot 10^{-5}$	$2.9 \cdot 10^{-5}$

order of magnitude. Sample No. 3 shows a gradual decrease toward (333), which intensifies down to the depth of (444). The pattern for sample No. 4 is fundamentally different: a gradual decrease toward (333) followed by an increase toward (444).

Regarding the concentration dependences of spherical clusters for samples No. 2 and No. 3, a sharp decrease toward (333) is observed, followed by an increase in values toward (444). For sample No. 4, the curve shows a monotonic decrease in concentration values. The general behaviour of the size dependences shares a common feature for all samples—the proximity of $R(\Lambda_{hkl})$ values for higher-order reflections. The scatter of cluster size values for the (111) reflection is explained by the influence of the disturbed surface layer, with the most favourable situation observed for sample No. 3. The anomalous deviation of the $R(\Lambda_{111})$ value can be attributed to the effects of mechanical surface treatment.

5. CONCLUSIONS

The defective structure of crystalline compounds was investigated using the total integrated reflectivity method based on the dynamical theory of x-ray diffraction. The most optimal combination of microdefects was identified during the simulation process: disk-shaped clusters (representing relatively large CdTe grains) surrounded by dislocation loops of corresponding sizes, and small spherical clusters (representing small CdTe grains) located in the spaces between the large grains. The dynamics of changes in the concentration and size of microdefects as a function of the extinction depth were demonstrated.

The general behaviour of $C(\Lambda_{hkl})$ and $R(\Lambda_{hkl})$ can be explained by the significant influence of the disturbed surface layer in all samples, as a

scatter in the size values of spherical microdefects is observed across all samples, while the range of concentration variations remains minimal. For the complex consisting of a disk-shaped microdefects and a dislocation loops, the dynamics of concentration and size changes are interconnected in samples Nos. 3 and 4. For sample No. 2, a significant deviation in sizes occurs. This can be attributed to the mosaic nature of the structure and the influence of the surface and grain boundaries, with the impact of the second one increasing with depth.

Overall, the considered model of the defective structure requires further supplementation with model microdefects that would allow for a better interpretation of grain boundary effects. Nevertheless, the proposed method for calculating the defective structure yields results that correlate well with the results of previous studies of these samples.

The authors are obliged to the Armed Forces of Ukraine for providing security that made it possible to carry out this work. This work was partially supported by the Ministry of Education and Science of Ukraine (grant No. 0125U000832, authors A. R. Kuzmin, M. S. Solodkyi; grant No. 0125U001483, authors I. M. Fodchuk, I. I. Hutsuliak, V. V. Dovganyuk, R. A. Zaplitnyy). This research was also supported by the National Academy of Sciences of Ukraine under contracts No. III-1-23 'Multiparametrical phase-variation diagnostics and modelling of electromagnetic properties of structures with inhomogeneously distributed imperfections'.

AUTHORS' CONTRIBUTIONS

V.B.M. generated key ideas, methodology, and analysis. I.M.F.: conceptualization; formulation and development of overarching research goals and aims; preparation, creation, and presentation of the manuscript, specifically writing the initial draft; provision of study materials, reagents, and research samples; data curation management. A.R.K.: preparation, creation, and presentation of the manuscript, specifically critical review, commentary, or revision, including prepublication stages; application of statistical, mathematical, computational, and other methods to analyse diffraction curves and experimental TIR curves. V.V.D.: modernization of the software suite (including programming code where necessary for data interpretation) for initial use in calculating microdefect concentrations and sizes. I.I.H.: preparation and creation of the manuscript, specifically x-ray diffractometry data processing (plotting and analysis of diffraction curves); primary translation of text. M.S.S.: preparation and creation of the manuscript, specifically x-ray diffractometry data processing (plotting and analysis of experimental TIR curves). R.A.Z.: modernization of the software suite (including programming code where neces-

sary for data interpretation) for subsequent reuse in calculating microdefect concentrations and sizes. Ya.D.G.: literature review; formatting/preparation of the theoretical section and references. V.V.L.: conceptualization; formulation or development of overarching research goals and aims; preparation, creation, and presentation of the published work, specifically editing the initial draft; provision of study materials; final editing of the manuscript. All authors gave final approval of the version to be published.

REFERENCES

1. V. B. Molodkin and E. A. Tikhonova, *Fiz. Met. Metalloved.*, **24**: 385 (1967) (in Russian).
2. V. B. Molodkin, S. I. Olikhovskii, and M. E. Osinovskii, *Metallofizika*, **5**: 3 (1983) (in Russian).
3. V. B. Molodkin, S. I. Olikhovskii, and M. E. Osinovskii, *Metallofizika*, **5**: 112 (1983) (in Russian).
4. V. B. Molodkin, S. I. Olikhovskii, E. N. Kislovskii, E. G. Len, and E. V. Pervak, *phys. status solidi (b)*, **227**: 429 (2001).
5. M. A. Krivoglaz, *Diffuznoe Rasseyanie Rentgenovskikh Luchey i Neitronov na Fluktuatsionnykh Neodnorodnostyakh v Neideal'nykh Kristallakh* [Diffuse Scattering of X-Rays and Neutrons on Fluctuation Inhomogeneities in Non-Ideal Crystals] (Kiev: Naukova Dumka: 1984) (in Russian).
6. M. A. Krivoglaz, *Diffraction of X-Rays and Thermal Neutrons in Imperfect Crystals* (Berlin–Heidelberg: Springer: 1992).
7. V. M. Pylypiv, T. P. Vladimirova, I. M. Fodchuk, B. K. Ostafiychuk, Ye. M. Kyslovskyy, V. B. Molodkin, S. I. Olikhovskii, O. V. Reshetnyk, O. S. Skakunova, V. V. Lizunov, and O. Z. Garpul', *phys. status solidi (a)*, **208**: 2558 (2011).
8. V. B. Molodkin, S. I. Olikhovskii, S. V. Dmitriev, A. I. Nizkova, and V. V. Lizunov, *Acta Cryst. A*, **76**: 45 (2020).
9. V. B. Molodkin, S. I. Olikhovskii, S. V. Dmitriev, and V. V. Lizunov, *Acta Cryst. A*, **77**: 433 (2021).
10. V. V. Lizunov, V. B. Molodkin, S. V. Lizunova, N. G. Tolmachev, O. S. Skakunova, S. V. Dmitriev, B. V. Sheludchenko, S. M. Brovchuk, L. M. Skapa, R. V. Lekhnyak, V. V. Molodkin, and K. V. Fuzik, *Progress in Physics of Metals*, **15**, Iss. 2: 55 (2014) (in Russian).
11. V. V. Lizunov, V. B. Molodkin, S. V. Lizunova, N. G. Tolmachev, E. S. Skakunova, S. V. Dmitriev, B. V. Sheludchenko, S. M. Brovchuk, L. N. Skapa, R. V. Lekhnyak, and E. V. Fuzik, *Metallofiz. Noveishie Tekhnol.*, **36**, No. 7: 857 (2014) (in Russian).
12. V. V. Lizunov, S. M. Brovchuk, A. I. Nizkova, V. B. Molodkin, S. V. Lizunova, B. V. Sheludchenko, A. I. Grankina, I. I. Rudnitska, S. V. Dmitriev, M. G. Tolmachev, R. V. Lekhnyak, L. M. Skapa, and N. P. Irkha, *Metallofiz. Noveishie Tekhnol.*, **36**, No. 9: 1271 (2014) (in Russian).
13. S. I. Olikhovskii, V. B. Molodkin, E. G. Len, E. S. Skakunova, and S. V. Lizunova, *Phys. Rev. B*, **99**: 235304 (2019).
14. V. B. Molodkin, H. I. Nyzkova, V. V. Lizunov, N. G. Tolmachev, S. V. Dmitriev,

L. I. Makarenko, O. V. Reshetnik, T. P. Vladimirova, Ya. V. Vasylyk, and I. N. Zabolotnyy, *Metallofiz. Noveishie Tekhnol.*, **41**, No. 12: 1677 (2019) (in Russian).
15. V. B. Molodkin, H. I. Nyzkova, V. V. Lizunov, A. O. Bilots'ka, L. I. Makarenko, T. P. Vladimirova, O. V. Reshetnyk, Ya. V. Vasylyk, and Ye. A. Tsapko, *Metallofiz. Noveishie Tekhnol.*, **44**, No. 4: 595 (2020) (in Ukrainian).
16. V. B. Molodkin, V. Yu. Storizhko, V. P. Kladko, V. V. Lizunov, A. I. Nizkova, O. Yo. Gudymenko, S. I. Olikhovskii, M. G. Tolmachev, S. V. Dmitriev, I. I. Demchyk, E. I. Bogdanov, and B. I. Hinko, *Semiconductor Physics, Quantum Electronics and Optoelectronics*, **24**, No. 1: 5 (2021).
17. V. B. Molodkin, V. Yu. Storizhko, V. P. Kladko, V. V. Lizunov, A. I. Nizkova, O. Yo. Gudymenko, S. I. Olikhovskii, M. G. Tolmachev, S. V. Dmitriev, I. I. Demchyk, E. I. Bogdanov, and B. I. Hinko, *Semiconductor Physics, Quantum Electronics and Optoelectronics*, **26**, No. 1: 17 (2023).
18. I. Fodchuk, A. Kuzmin, I. Hutsuliak, M. Solodkyi, V. Dovganyuk, O. Maslyanchuk, Y. Roman, R. Zaplitnyy, O. Gudymenko, V. Kladko, V. Molodkin, and V. Lizunov, *Proc. of SPIE*, **11369**: 113691H (2020).
19. O. Maslyanchuk, I. Fodchuk, M. Solovan, I. Boledzyuk, A. Kuzmin, V. Gnatyuk, and T. Aoki, *Proc. of SPIE*, **12126**: 121260K (2021).
20. I. M. Fodchuk, A. R. Kuzmin, O. L. Maslyanchuk, I. I. Hutsuliak, M. S. Solodkyi, Yu. T. Roman, M. M., Solovan, and O. Yo., Gudymenko, *Phys. Chem. Solid State*, **23**, No. 1: 144 (2022).
21. I. M. Fodchuk, A. R. Kuzmin, I. I. Hutsuliak, M. D. Borcha, and V. O. Kotsyubynsky, *Semiconductor Physics, Quantum Electronics and Optoelectronics*, **26**, No. 4: 415 (2023).
22. I. M. Fodchuk, A. R. Kuzmin, I. I. Gutsuliak, M. S. Solodkyi, O. L. Maslyanchuk, Yu. T. Roman, V. P. Kladko, O. Yo. Gudymenko, V. B. Molodkin, and V. V. Lizunov, *Metallofiz. Noveishie Tekhnol.*, **43**, No. 10: 1289 (2021) (in Ukrainian).
23. V. V. Brus, O. L. Maslyanchuk, M. M. Solovan, P. D. Maryanchuk, I. M. Fodchuk, V. A. Gnatyuk, N. D. Vakhnyak, S. V. Melnychuk, and T. Aoki, *Sci. Rep.*, **9**, No. 1: 1065 (2019).
24. O. Maslyanchuk, M. Solovan, V. Brus, P. Maryanchuk, E. Maistruk, I. Fodchuk, and V. Gnatyuk, *Nucl. Instrum. Methods Phys. Res. A*, **988**: 164920 (2021).
25. H. Shiraki, M. Funaki, Y. Ando, A. Tachibana, S. Kominami, and R. Ohno, *IEEE Trans. Nucl. Sci.*, **56**, Iss. 4: 1717 (2008).
26. H. Shiraki, M. Funaki, Y. Ando, S. Kominami, K. Amemiya, and R. Ohno, *IEEE Trans. Nucl. Sci.*, **57**, Iss. 1: 395 (2010).
27. V. B. Molodkin, H. I. Nyzkova, V. V. Lizunov, V. V. Molodkin, S. V. Dmitriev, L. I. Makarenko, O. S. Kononenko, I. I. Demchyk, and N. P. Irkha, *Metallofiz. Noveishie Tekhnol.*, **40**, No. 9: 1133 (2018) (in Russian).
28. V. B. Molodkin, S. I. Olikhovskii, E. G. Len, Ye. M. Kyslovskyy, O. V. Reshetnyk, T. P. Vladimirova, B. V. Sheludchenko, E. S. Skakunova, V. V. Lizunov, E. V. Kochelab, I. M. Fodchuk, and V. P. Klad'ko, *Metallofiz. Noveishie Tekhnol.*, **38**, No. 1: 99 (2016).
29. V. V. Lizunov, V. B. Molodkin, S. I. Olikhovskiy, S. V. Lizunova, N. G. Tolmachev, A. I. Nizkova, E. S. Skakunova, S. V. Dmitriev, B. V. Sheludchenko, T. G. Sych, E. V. Fuzik, R. V. Lekhnyak, and L. N. Skapa,

Metallofiz. Noveishie Tekhnol., **37**, No. 2: 265 (2015) (in Russian).
30. V. V. Dovganyuk, I. M. Fodchuk, O. G. Gymchynsky, A. V. Oliynych-Lysyuk, Ye. M. Kyslovs'ky, A. O. Bilots'ka, T. P. Vladimirova, R. F. Seredenko, and Z. Swiantek, *Metallofiz. Noveishie Tekhnol.*, **28**, No. 10: 1291 (2006) (in Russian).